Journal of Structural Geology, Vol. 7, No. 6, pp. 701 to 712, 1985
Printed in Great Britain

0191-8141/85 $03.00 + 0.00

Faults and associated fault rocks of the Southern Arunta block, Alice Springs, Central Australia

H. K. OBEE and S. H. WHITE

Department of Geology, Imperial College, London SW7 2BP, U.K.

(*Received* 31 *July* 1984; *accepted in revised form* 14 *February* 1985)

Abstract—The Southern Arunta block within the Alice Springs region is dissected by an E–W-trending network of high-angle reverse faults. Microstructural evidence indicates that there is a change from dominantly ductile to brittle faulting southwards across the block towards the Amadeus Basin, and this suggests that the faults in the north were progressively uplifted by the more southern faults. The generation of ultramylonite has been particularly extensive in the Alice Springs region. TEM and SEM observations have allowed an appraisal of the deformation mechanisms at ultrafine grainsizes and suggest complex interactions between dislocation processes, diffusion and grain-boundary sliding.

INTRODUCTION

THE GEOLOGY of the Alice Springs region (Fig. 1) is dominated by faulted basement rocks of the Proterozoic Arunta block overlain unconformably in the south by the late Proterozoic to Palaeozoic sediments of the Amadeus Basin sequence (Offe & Shaw 1983, Shaw & Wells 1983). The Arunta block has undergone an extended Proterozoic history of tectono-metamorphic events prior to the deposition of the cover sediments. These began with the 1800 Ma Strangeways Event, noted for granulite-facies metamorphism (Iyer *et al.* 1976, Black *et al.* 1983); and was followed by the Aileron (1700–1650 Ma), Anmatjira (1400 Ma) and Ormiston (1050–900 Ma) Events (Black *et al.* 1983). Subsequent to the deposition of the Amadeus Basin sediments, further deformation occurred in the Alice Springs Orogeny, dated at 335–312 Ma (Armstrong & Stewart 1975). During this orogeny, earlier zones of weakness, which include the Redbank Deformed Zone in the area studied, were reactivated (Marjoribanks 1974, Offe & Shaw 1983) and granulites to the north of the Redbank Deformed Zone were thrust southwards. Displacements along the Redbank Deformed Zone and faults to the south resulted in basement-cored nappes being thrust southwards over the Amadeus sediments. It is these faults that will now be considered in detail.

The distribution of faults in the Alice Springs region is shown in Fig. 1. They form an E–W-trending anastomosing network which defines a series of kilometric-scale blocks or fault slices, although on a finer scale these blocks are also sheared by less prominent faults. Generally all faults dip steeply N and display a reverse sense of movement. The grade of metamorphism in the country-rock gneisses changes across the major fault in the region, the Redbank Deformed Zone, so that granulites or partially retrogressed granulites crop out to the north, and amphibolite-grade rocks to the south.

The characteristic fault rocks in the region are mylonites and mylonitic gneisses to the north, and c-type mylonites and cataclasites to the south. The matrix of the fault rocks in the north, outcropping within the Redbank Deformed Zone, display upper greenschist-facies metamorphic mineral assemblages, e.g. quartz + feldspar + biotite + garnet, whilst the matrix of southern fault rocks exhibit lower greenschist-facies assemblages; for example quartz + biotite + muscovite + chlorite. To illustrate this gradational southward change, selected examples have been taken from the localities marked A–G on Fig. 1 for detailed microstructural studies. Observations are divided into three sections: the Redbank Deformed Zone, faults between the Redbank and Charles River Fault Zones and the Charles River Fault Zone. Regional observations are based on detailed mapping of selected areas and on two detailed traverses: from New Well to the south, and a N–S traverse through Alice Springs along the Stuart Highway.

REDBANK DEFORMED ZONE

The Redbank Deformed Zone is an E–W-trending belt of highly deformed rocks (Marjoribanks 1974) that crops out in a series of hills in the north of the Alice Springs region. In the west of the studied area the exposed width is up to 3 km, but it becomes narrower to the east (1.5 km). The characteristics of the zone are a steeply N-dipping schistose mylonitic foliation, with an associated extension lineation that plunges down dip (see Fig. 2a). Minor fold axes within the foliation plunge parallel to the extension lineation. The schistose mylonitic fabric heterogeneously overprints earlier intermediate–basic migmatitic gneisses to varying degrees, but usually it is so pervasive that it completely obliterates earlier textures within the zone. However it does contain less reworked pods (usually 5–50 m in length) of migmatite in which episodes of remobilization and complex fold interference patterns can be recognized.

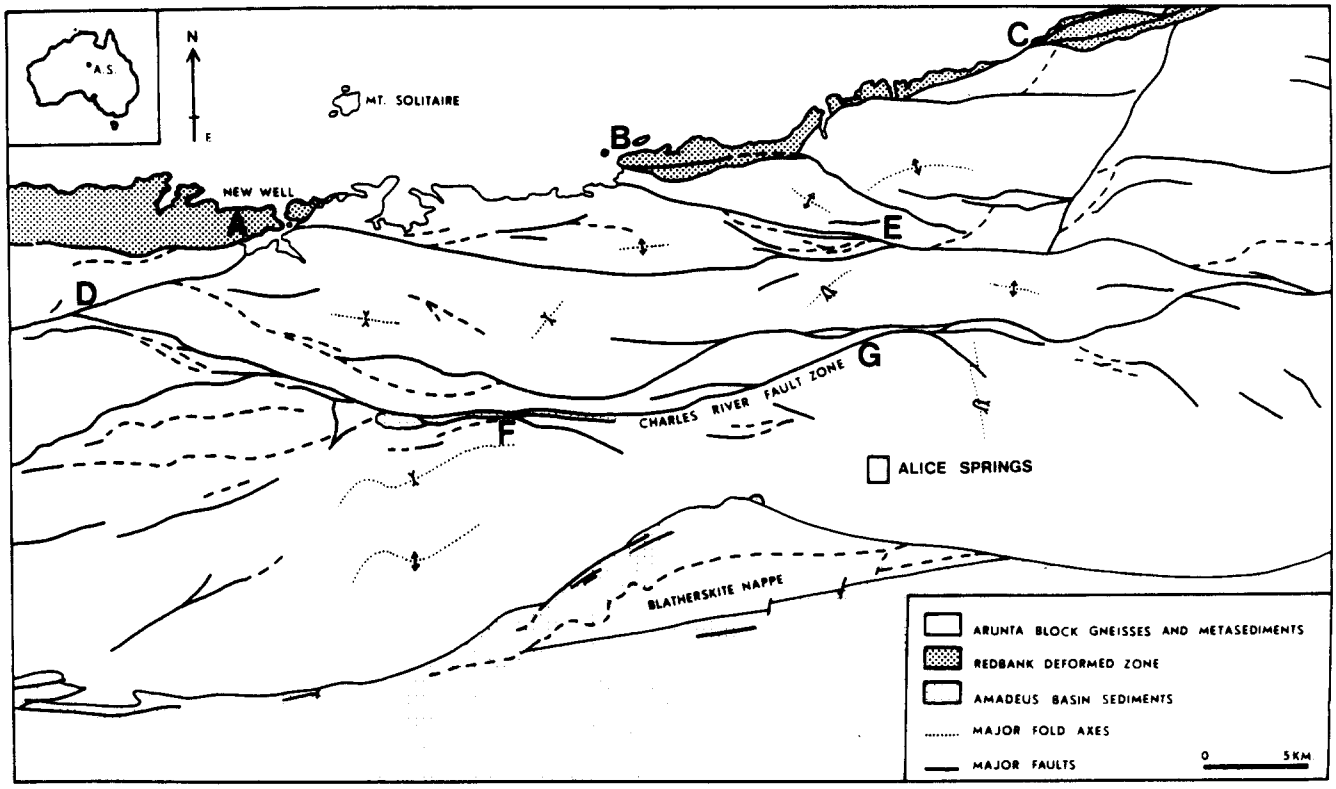

Fig. 1. The distribution of faults in the Alice Springs region, modified from the BMR 1:100,000 Alice Springs geological sheet. Localities A–G refer to samples described in text.

The mineralogy of the schistose mylonites is varied, although a typical assemblage includes quartz, feldspar, biotite, hornblende ± garnet, and accessory minerals. In the field they exhibit an augen texture with large feldspars (up to 8 cm in diameter) sitting in a fine-grained matrix, which ranges from 10 to 1000 μm in grainsize (see Fig. 3a). In thin section the feldspars show internal strain features such as undulose extinction and deformation lamellae, as well as recrystallisation around their margins, and occasional shear fractures. Likewise quartz grains are highly strained, producing subgrain structures and deformation bands. In the quartz-rich mylonites a strong optical preferred orientation is developed (Fig. 2b), characterized by type I girdles (Lister 1977) with sense of asymmetry consistent with a reverse sense of movement. The quartz grains have an oblique shape fabric similar to that reported in many mylonite zones (Brunel 1980, Evans & White 1984). The obliquity is again consistent with a reverse sense of movement. Garnet and hornblende in these mylonites usually exhibit fractures, which give rise to irregularly shaped grains.

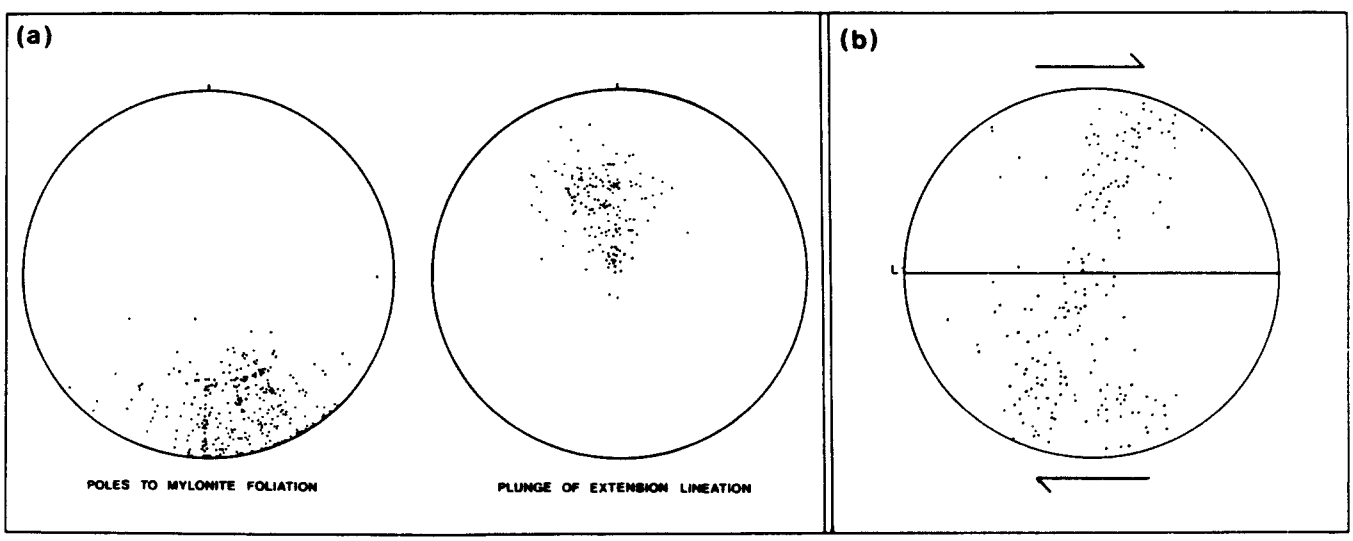

Fig. 2. Structural data. (a) Lower hemisphere equal-area projections of poles to mylonitic foliation and plunge of extension lineation within the Redbank Deformed Zone. (b) Asymmetric quartz *c*-axis fabric from a quartz vein within the Redbank Deformed Zone. Lineation (L) plunges north. Number of measurements = 200.

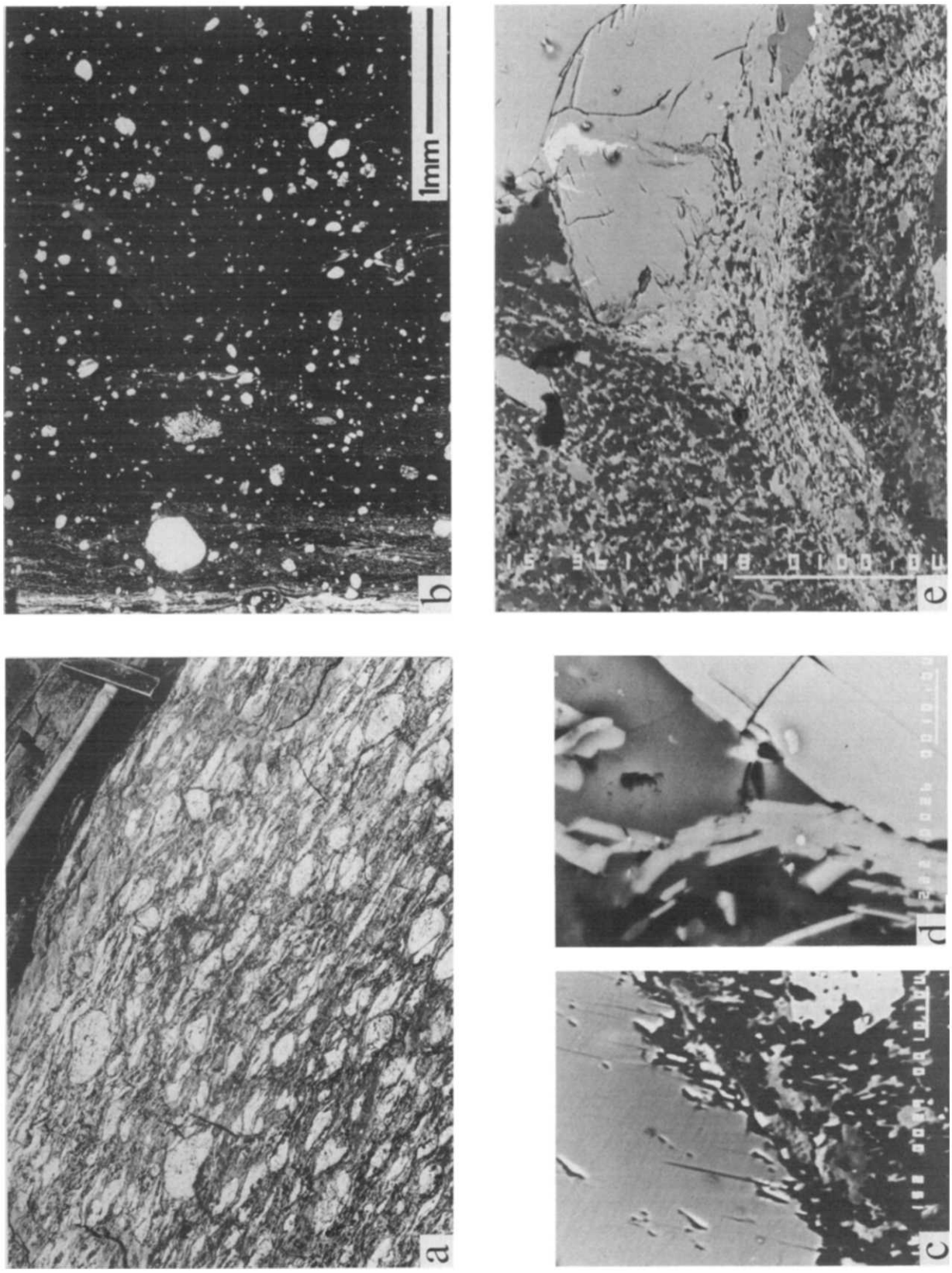

Fig. 3. Redbank Deformed Zone mylonites. (a) Field photograph of a typical schistose mylonite. (b) Optical micrograph of an ultramylonite viewed with crossed nicols. Porphyroclasts of feldspar, garnet and hornblende within an ultrafine black matrix. (c) Back-scattered SEM micrograph showing a hornblende porphyroclast with stepped cleavage planes which are the sites for the growth of biotite. Scale bar = 10 μm. (d) Newly formed biotite, parallel to cleavage in the hornblende, in the process of being rotated off into the matrix. Scale bar = 10 μm. (e) Hornblende porphyroclast within mylonite displaying kinking and micro-fracturing. The small fractured fragments are pulled out into the matrix. Scale bar = 100 μm.

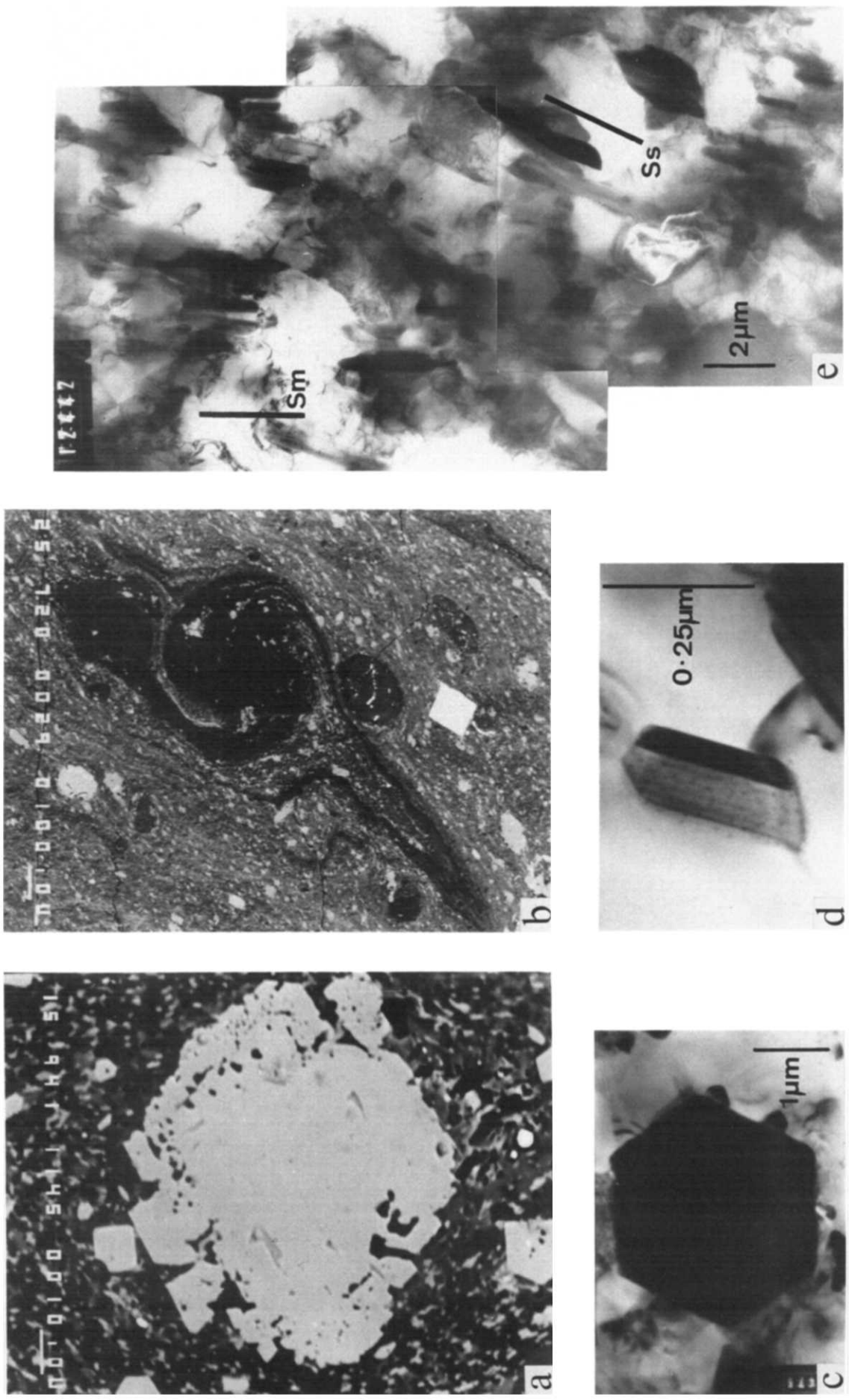

Fig. 5. Electron micrographs from the ultramylonites. (a) Back-scattered SEM micrograph of garnet growth over the ultrafine matrix. Scale bar = 10 μm. (b) Back-scattered SEM image of a plagioclase porphyroclast with folded recrystallized tails. Scale-bar = 100 μm. (c) TEM micrograph showing a euhedral garnet of the matrix measuring approximately 2 μm. (d) TEM micrograph of a biotite grain of the matrix measuring 0.25 μm in length. (e) TEM micrograph showing two orientations of biotite, representing the mylonite foliation (S_m) and micro-shear band foliation (S_s).

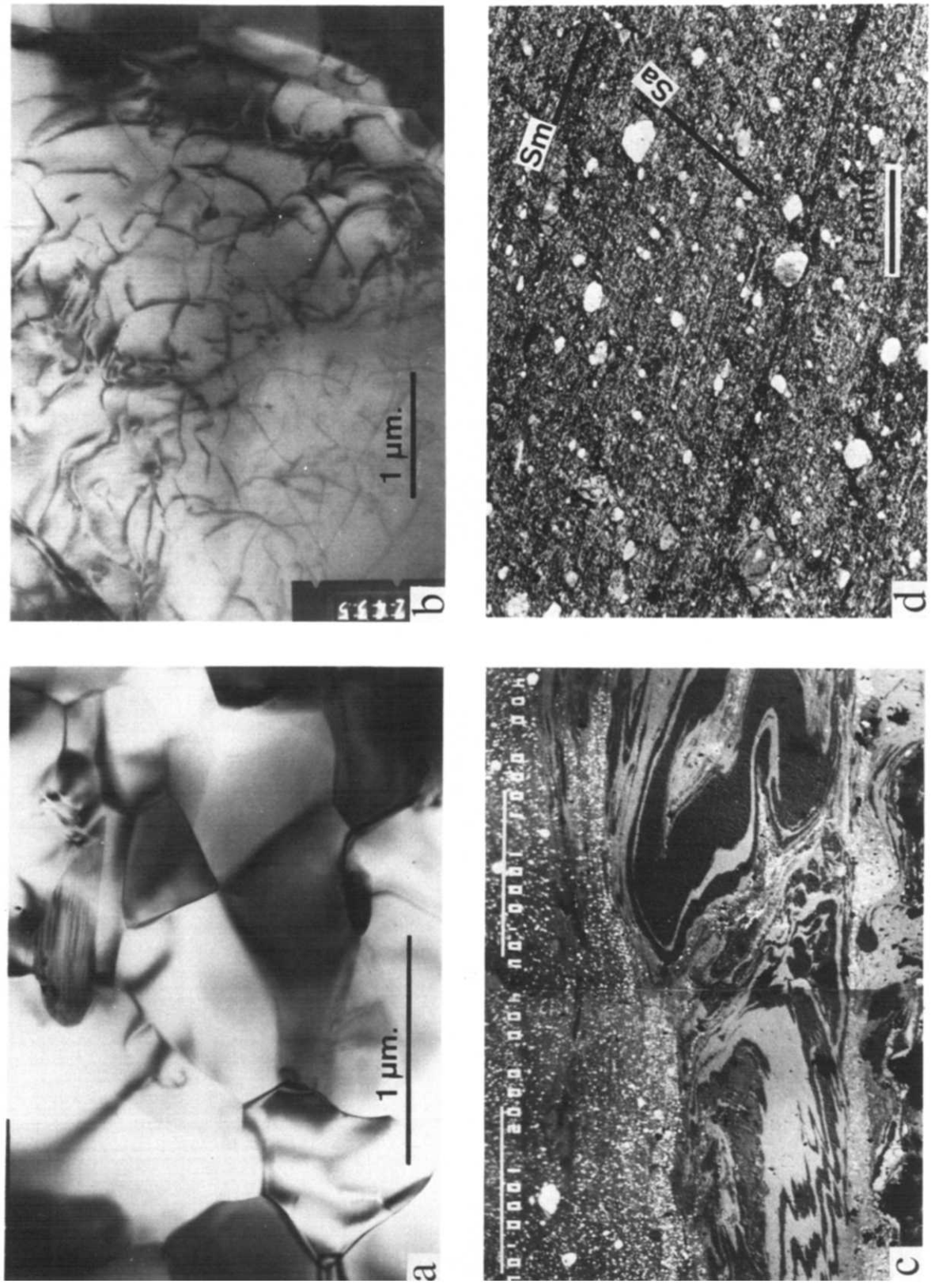

Fig. 6. Mylonite and ultramylonite microstructures. (a) TEM micrograph of cluster of quartz grains approximately 1 μm in width free from dislocations. (b) TEM micrograph of a quartz grain, approximately 5 μm wide, displaying a high dislocation density. (c) Back-scattered SEM micrograph showing extreme ductile working of quartz (black phase), plagioclase (intermediate grey) and alkali feldspar (light grey) from a mylonite adjacent to an ultramylonite band (seen at the top of the micrograph). The ultramylonite band contains stable garnet (bright phase). Scale bar = 1000 μm. (d) Optical micrograph viewed under crossed nicols illustrating the 'apparent foliation' (S_a) with respect to the mylonite foliation (S_m).

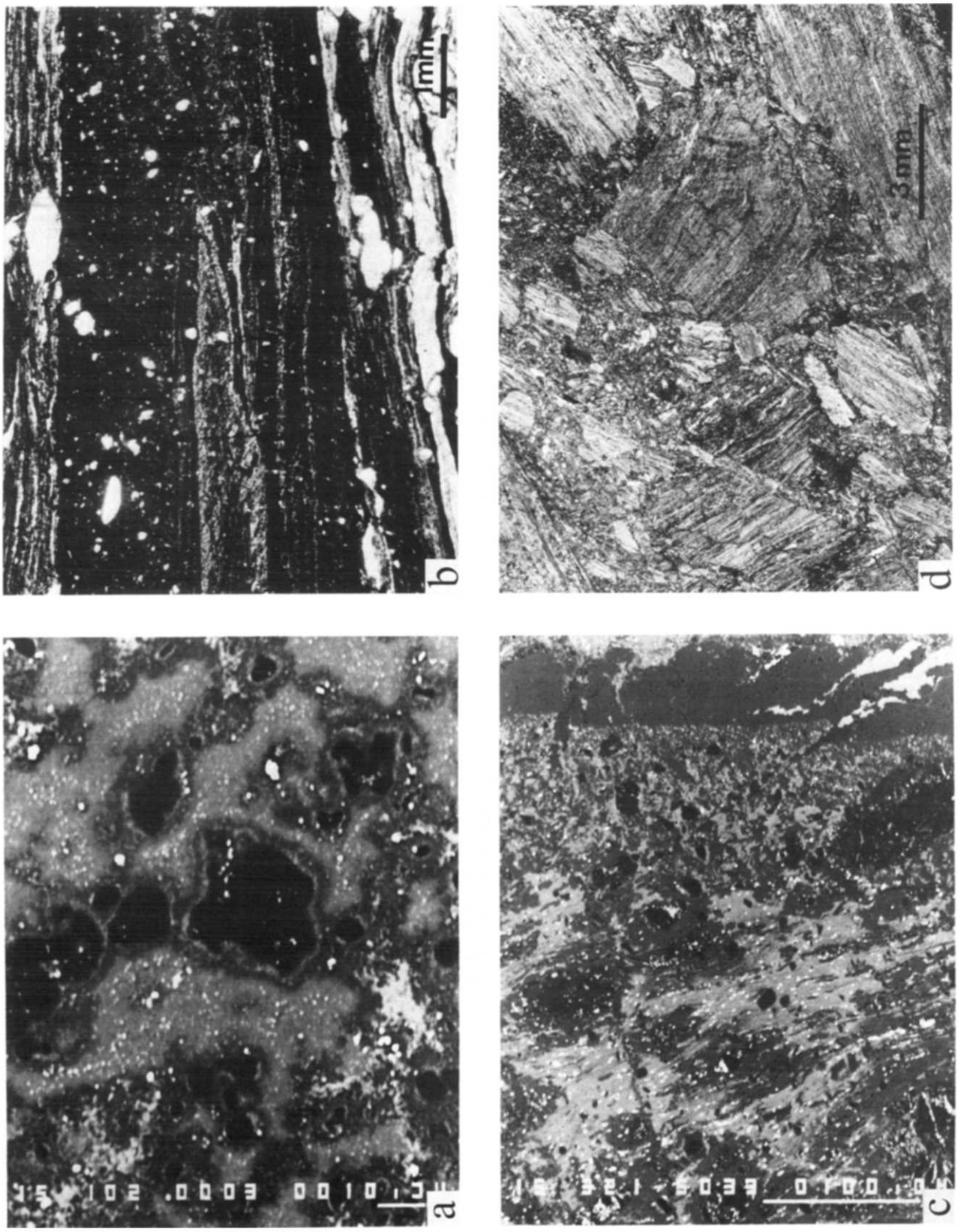
1mm
b
3mm
d
a
c

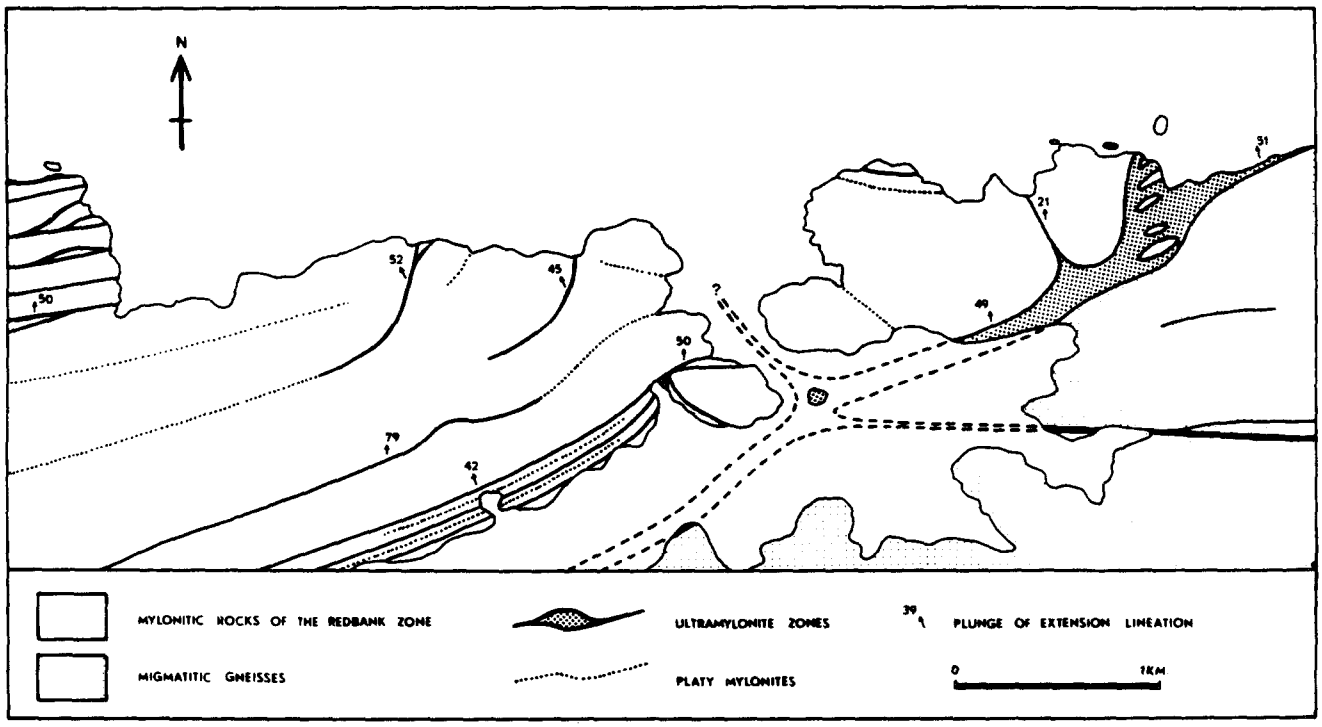

Fig. 4. Sketch map of the main ultramylonite zones within the New Well area (locality A Fig. 1). Note the constant lineation orientation in both the NE–SW and E–W trending zones.

The sense of shear within the Redbank Deformed Zone can be determined from several sources, and include both field and microstructural data. Displaced markers are rare, so that the following criteria, which have been widely employed to determine fault movement (see White 1982, Passchier 1983, Simpson & Schmidt 1983), are used: shear bands, asymmetric folds, asymmetric tails around feldspar augen, shear fractures and asymmetric quartz *c*-axis fabrics (Fig. 2b). In addition an oblique 'apparent foliation', which will be discussed later, was used. All of these sources indicate a consistent reverse sense of movement within the zone.

Within the schistose mylonitic foliation, and usually concordant with it, are zones of more intense strain which manifest themselves as either strong platy mylonites or as ultramylonite bands.

Platy mylonites

The platy mylonites are zones of high strain that are often preferentially eroded to form gullies within the topographic ridges. Their width is usually 0.25–10 m and their margins are diffuse. These rocks are characterised by an abundance of biotite which gives them a platy appearance in the field. The grainsize is smaller than the surrounding schistose mylonite, but grains exhibit optical strain features similar to those described earlier. Although these zones are considered to be regions of high strain, they have not undergone the extreme grain refinement of the ultramylonites, where deformation is considered more concentrated.

Ultramylonites

More common than the platy mylonites are the ultramylonites which vary in width from less than 1 cm to several metres. In contrast to the platy mylonites these zones have sharper margins, and display little evidence for a gradual strain gradient into the schistose mylonites. The change from schistose mylonite to ultramylonite occurs within the space of a few millimetres. In some areas, such as around Mount Forster (locality B, Fig. 1), the zones appear to be anastomosing, whilst in other areas such as New Well (locality A, Fig. 1) they form a more ordered pattern with interconnecting reverse-slip and oblique strike-slip zones. Figure 4 shows a sketch map of the ultramylonites at New Well and illustrates the constant plunge in lineation in both E–W and NE–SW oriented zones.

Fig. 9. Cataclasite and pseudotachylyte microstructures from faults between the Redbank Deformed Zone and the Charles River Fault Zone and ultracataclasite microstructure from the Charles River Fault. (a) Back-scattered SEM image of pseudotachylyte showing rimmed structures: cores of quartz surrounded firstly by biotite, then plagioclase and finally alkali feldspar. Scale bar = 10 μm. (b) Optical view of an isoclinal flow fold in pseudotachylyte. The pseudotachylyte vein (black rock in the centre of micrograph) is parallel to the mylonitic foliation. (c) Back-scattered SEM micrograph of an ultracataclasite vein with a well-developed oblique foliation in the centre and randomly orientated grains at the margin (on the right of the micrograph) scale bar = 100 μm. (d) Optical view of an ultramylonite reworked to form a cataclasite.

Ultramylonite microstructure

The most noticeable characteristic of the ultramylonites is the ultrafine grainsize which is usually less than 5 μm and commonly between 1 and 3 μm. Because of this fine grainsize standard optical analytical techniques are inadequate, so a study has been undertaken using back-scattered electron imagery in a Jeol 733 SEM Superprobe and an AE1 EM7 high voltage TEM. The specimen preparation techniques used in both are described in White *et al.* (1984) and Barber (1970), respectively. These techniques allow accurate grainsize measurement, phase identification and chemical characterisation as well as an insight into the deformation mechanisms that were operative during fault movement.

As in the mylonites, the mineralogy of the ultramylonites is varied, although generally the more northern and western ultramylonite exposures within the Redbank Deformed Zone contain porphyroclasts of hornblende, garnet and feldspar in a matrix of quartz, feldspar, biotite and newly recrystallised garnet. The more southern and eastern exposures generally contain feldspar porphyroclasts in a matrix of quartz, feldspar, biotite and epidote. Figure 3(b) shows a typical optical view of an ultramylonite with a dark fine-grained matrix containing porphyroclasts of hornblende, garnet and feldspar.

The ultramylonites are considered to have undergone extensive strain softening, and they show evidence for considerable grain size reduction; i.e. the gneisses had their grainsize reduced firstly to that of a schistose mylonite and then locally to that of an ultramylonite. Evidence for some of the mechanisms involved in grainsize reduction and recrystallisation of the different phases is visible in the porphyroclasts, so these will now be described for each mineral in turn.

Amphibole. The hornblende porphyroclasts within an ultramylonite collected at locality B (Fig. 1) display considerable evidence for reaction-enhanced ductility (see White & Knipe 1978), involving both metamorphic and deformational processes. When viewed optically the hornblende appears as elongate grains with rounded margins, with the long axis parallel to the mylonite foliation. In the few clasts which have their long axis perpendicular to the foliation axial fractures have developed, and ilmenite, quartz and epidote have grown along them. More commonly, however, the hornblende is free from fracturing and displays little evidence of internal strain features. Back-scattered electron imagery, at high magnification, shows that the hornblende is not rounded, but is stepped along the cleavage planes (Fig. 3c). Microprobe analysis has shown that these steps were sites for the growth of biotite and to a lesser extent quartz and epidote. Once the biotite had grown (usually to a grainsize of between 1 and 10 μm) it was mechanically rotated and plucked into the matrix of the ultramylonite (Fig. 3d), which is devoid of amphibole.

From the microstructural observations cited above, it appears that most of the strain in the hornblende clasts was taken up in zones of crystallization of new mineral phases along cleavage planes. This process is likely to have aided the softening within the ultramylonite, for it produced small strain-free grains along with a weaker assemblage. It also resulted in porphyroclasts of smaller dimensions. This mechanism for grain refinement provides a contrast to that of the hornblende in the mylonite outside the ultramylonite band, where the dominant process is microcracking (Fig. 3e).

Garnet. Unlike the hornblende, the garnet porphyroclasts were reduced in grainsize by brittle failure. After the development of an irregular network of fractures, small sub-angular fragments were pulled out along the foliation. Grain-refinement processes in the garnets are slightly confused by the fact that some of the fragments show minor post-tectonic growth. Euhedral faces have grown over the matrix to form zones of fine inclusions. The rims of newly grown garnet tend to be richer in Ca than the old grains and relatively depleted in Mn and Fe. There is no evidence for syn-tectonic growth of garnet from rotation fabrics, and the growth is interpreted to be due to metamorphism outlasting the deformation. Figure 5(a) is a back scattered electron micrograph of a post-tectonically grown garnet (diameter 80 μm) containing small inclusions within the rim.

Feldspar. The large feldspar augen are reduced in grainsize by the production of subgrains around their margin, so that a core and mantle structure has developed (White 1976). Recrystallization has occurred and the newly formed grains were pulled out into long tails. Microanalysis of the recrystallized grains reveals a change in chemical composition; in the case of plagioclase the recrystallized grains are depleted in Ca. The newly formed tails were not immediately assimilated into the matrix, but due to the inhomogeneity of the matrix set up by the density of porphyroclasts, began to form asymmetric folds under continuing deformation. If the shearing of the tails was accompanied by rotation of the host feldspar then complex patterns arose, as illustrated in Fig. 5(b). Eventually the folds were sheared out, and the tails assimilated into the matrix, leaving porphyroclasts of smaller dimensions.

Matrix. The matrix of an ultramylonite taken from locality B (Fig. 1) consists of quartz, feldspar, garnet, and biotite. The micrographs in Figs. 5(c)–(e) show these phases. Note the fine grainsize of these minerals with euhedral garnet approximately 2 μm in diameter and biotite on the sub-μm scale. The quartz grains of the matrix display varying densities of dislocations. The relatively large grains (approximately 5 μm) have high dislocation densities (5×10^8) whilst those of approximately 1 μm tend to be dislocation free. The cut-off point at which no dislocations are visible is between 1.5 and 2.0 μm. Figure 6(a) shows dislocations in a quartz grain that is approximately 5 μm in diameter, whereas Fig. 6(b) displays a cluster of dislocation-free grains each of which is approximately 1 μm in diameter. Very rarely

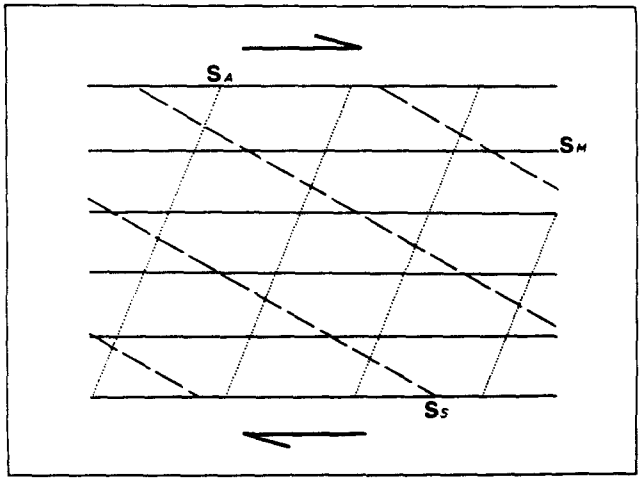

Fig. 7. The relationship among the mylonite foliation (S_m), micro-shear band foliation (S_s) and 'apparent foliation' (S_a) in a biotite-rich ultramylonite.

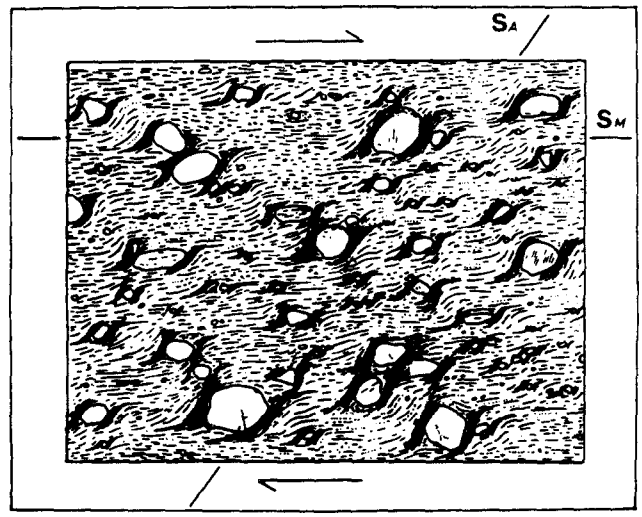

Fig. 8. Schematic diagram illustrating the development of an 'apparent foliation' (S_a) by the deflection of biotite around numerous porphyroclasts. S_m, mylonitic foliation.

is the matrix of the ultramylonites free from porphyroclasts. This suggests that after a certain level of grain refinement most of the strain can be taken up within the matrix, and the remaining porphyroclasts act as passive inclusions.

There is a series of ultramylonite bands that, as will be discussed later, are considered not to have formed by the grainsize-reduction mechanisms described above but by the reworking of pseudotachylytes, as reported by Passchier (1982). These bands are usually discordant with the mylonite foliation, are very thin (on the cm scale) and have a particularly fine grainsize. It is these bands that have the sharpest margins, the change between mylonite and ultramylonite taking place within several μm. The mylonite adjacent to the band often displays extreme ductile working and Fig. 6(c) shows fine-scale folds in such an area involving quartz, alkali feldspar and plagioclase. The micrograph also shows that garnet (bright phase) is present in the ultramylonite.

FAULT ZONES BETWEEN THE REDBANK DEFORMED ZONE AND CHARLES RIVER FAULT

The faults south of the Redbank Deformed Zone are marked by narrower (up to 15 m) ultramylonite and mylonite zones. Although ductile processes dominate most of these fault rocks, brittle processes are increasingly important along with the role of fluids. The interaction of brittle and ductile processes and retrogressive metamorphism can be seen in rocks of the Colyer Creek Fault (south of locality E, Fig. 1), exposed in the creek to the east of the Stuart Highway. Within the fault rocks south of the Redbank Deformed Zone garnet and amphibole are absent, although they are present in the host gneisses, and the mineralogy is dominated by epidote and biotite along with quartz and feldspar.

Ultramylonites

An example of an ultramylonite south of the Redbank Zone is taken from locality D (Fig. 1). Here the rock is dominated by biotite, which defines three foliations. These are the mylonitic foliation (S_m), which is the dominant planar fabric in the rock, a micro-shear band foliation (S_s) and an oblique 'apparent foliation' (S_a). The relationship among the three is illustrated in Fig. 7 and the latter two are discussed below.

The micro-shear-band foliation is considered to be a fine-grained equivalent to the extensional crenulation cleavage structures described by Platt & Vissers (1980). Small displacements of markers indicate extension along the older foliation. TEM analysis reveals the shear bands to be made up of small biotite grains (5 μm long). Two distinct populations of biotite are observed, one in an orientation representing the mylonitic foliation and the other the shear-band foliation. This is shown in Fig. 5(e). The micro-shear-band foliation makes an angle of about 30° with the mylonitic foliation and the sense of shear determined from these structures is a reverse movement, again suggesting north side up.

The 'apparent foliation' develops at a high angle to the mylonitic foliation, in some cases almost perpendicular to it. This foliation is not considered to be a conjugate foliation to the micro-shear-band foliation because (a) only two orientations of mica were observed in the matrix away from any porphyroclasts during TEM analysis and (b) it is only noticeable in areas with a high density of porphyroclasts. It is therefore considered to develop as a result of the deflection of biotite grains around the porphyroclasts, so that when viewed optically the alignment of micas around several porphyroclasts creates an 'apparent foliation'. Figure 6(d) illustrates an 'apparent foliation' at a high angle to the mylonitic fabric, defined by domains in which biotite is orientated in a position for optical extinction. The orientation of this apparent foliation is a reliable sense of shear indicator within biotite-rich ultramylonites, and as can be seen from Fig. 8, is related to the asymmetry of the foliation around individual porphyroclasts.

Pseudotachylytes

South of the Redbank Zone greater amounts of unreworked pseudotachylytes occur. Figure 9(a) shows a back scattered SEM image of a devitrified pseudotachylyte from locality D (Fig. 1). The micrograph reveals that rimmed structures have nucleated on cores of quartz (black phase). Around the quartz is a fine envelope of biotite (bright phase), followed by plagioclase (dark grey) and alkali feldspar (light grey). Although no foliation has developed, a strong mineralogical banding is evident when viewed optically, which has locally been folded into tight isoclinal folds by viscous flow (Fig. 9b). Microanalysis of the banding has shown it to be a compositional change from dominantly alkali feldspar to plagioclase.

CHARLES RIVER FAULT ZONE

The Charles River Fault Zone comprises the Charles River Fault, the major fault in the south of the region which thrusts basement gneisses over Amadeus Basin sediments, along with many bedding-parallel thrusts in the sediments. The geometry of these thrusts indicates displacement towards the south, and they are well exposed in Heavitree Quartzite ridges at Simpsons Gap (locality F, Fig. 1) and westwards in the narrow outcrop of sediments. Here small-scale duplex structures are particularly well developed.

Whereas the Redbank Deformed Zone is dominated by ductile processes, the Charles River Fault is dominated by brittle deformation. Like the other faults it dips steeply 40–70°N and has a reverse sense of movement. In the field the fault appears to have a strong mylonitic foliation on the southern margin, with more pseudotachylytes and ultracataclasites on the northern margin of the mylonite and country rock. When viewed optically all the fault rocks appear to be dominated by brittle processes with the growth of new phases. White (1982) refers to mylonitic rocks dominated by such processes as c-type mylonites.

Within a mylonite from locality G (Fig. 1) the quartz grains exhibit undulose extinction, and some have been pulled out into ribbons, with fine-grained recrystallization around their margins. The feldspar deformation contrasts with this, in that fractures have developed perpendicular to the foliation. The foliation is enhanced by the growth of phyllosilicates (biotite, muscovite and chlorite). On the northern margin of the fault zone, the rocks display effects of cyclic brittle failure. Firstly the quartz grains have been fragmented, then biotite has grown between the displaced fragments, and further failure has caused kinking of the biotite cleavage. New biotite growth has finally occurred along the kinks. This process of repeated failure and mineral growth appears to have been important in the evolution of these rocks. It may be explained by mineral phases sealing fractures, which leads to work hardening and a build up of stress, which in turn leads to failure.

Ultracataclasite rocks within gneisses usually develop in irregularly shaped veins separating displaced blocks (approximately 1 cm). The matrix of the veins consists of angular to sub-angular fragments (between 3 and 100 μm). The mineral assemblage is quartz + feldspar + biotite + chlorite and a high percentage of iron oxide. Figure 9(c) shows that these ultracataclasites have a strong foliation, accentuated by the growth of biotite. The new foliation is oblique to the vein margin (Riedel shear of Hall 1983) and forms in the centre of the vein, for at the margin the grains remain randomly orientated. The micrograph also shows late microfaults causing small displacements of the vein, again illustrating the cyclicity of the brittle failure.

As within the Charles River Fault Zone, there are many minor faults in the Alice Springs region (mainly to the south) that display cataclastic and gouge-bearing fault rocks, containing mainly low-grade assemblages rich in chlorite and epidote.

EVIDENCE FOR FAULT REACTIVATION

Field observations in the Alice Springs region suggest that several of the faults have been reactivated. Marjoribanks (1974) suggested that the Redbank Deformed Zone had been reactivated. Field evidence for reactivation is rare but cross-cutting relationships between different mylonitic fault rocks do occur. One example is exposed at locality D (Fig. 1) where mylonitic gneisses (foliation dip 67–224°) with an oblique extension lineation (plunge 62–260°) are truncated by a later mylonite zone (dip 68–336°) with a down-dip lineation. Not only are the two distinguished by orientation, but the later mylonite is more fine-grained and has the lower-grade mineral assemblage discussed above. Figure 9(d) shows another example of reactivation from a fault south of the Redbank Deformed Zone, taken from a locality north of Colliers Creek (Locality E, Fig. 1) in a road cutting along the Stuart Highway.

Here an earlier ultramylonite, which where intact dips steeply S, has been reworked to form a cataclasite. Blocks of the original ultramylonite have been fragmented and rotated, and are surrounded by a fine-grained matrix. The observed microstructure suggests that this fault has been reactivated at a shallower crustal level. Reactivation along the Charles River Fault is inconclusive, although the variation in microstructure described above could be interpreted as reflecting different phases of movement, again with a shallowing of crustal level with time.

DISCUSSION

Sibson (1977) proposed a conceptual model for a major fault zone in which a zone of elastico-frictional behaviour overlies a quasi-plastic regime. The fault rocks produced in such a fault zone are dependent on the depth at which they formed in the crust. This is mainly

due to the response of quartz to deformation with increasing temperature (Sibson 1983). At high crustal levels gouge, breccias, cataclasites and pseudotachylytes are generated by seismogenic slip, and at depth mylonitic rocks are produced by aseismic shearing, with a complex interplay between brittle and crystal–plastic processes occurring where the two regimes overlap (White & White 1983).

The Alice Springs region of Central Australia exhibits a wide range of fault rocks, from near-surface gouges through to deep-level mylonites. The variation in microstructure and metamorphic grade of the fault rocks is interpreted as indicating fault activity at different levels in the crust. In the north of the region, for example, within the Redbank Deformed Zone, the fault rocks formed at middle to lower levels in the crust; whereas those to the south (e.g. the Charles River Fault) formed at higher crustal levels. The progressive change from deep to shallow level faulting might be explained by uplift of the deeper-level northerly mylonites to higher crustal levels along the more southerly faults. The evidence for reactivation along some of the deeper faults (e.g. the cataclasis of the mylonites) suggests that they were not entirely passive when being uplifted by the southern faults. The faults have segmented the basement into slices and, therefore, both translation and rotational components must be considered in correlation of deformational events between fault slices.

Within the Redbank Deformed Zone the structural observations cited above suggest that it represents a fundamental weakness in the earth's crust that has controlled the structural evolution of Central Australia over an extended period of geological time. Constraints on early phases of movement are difficult to achieve due to the pervasive reworking during the Alice Springs Orogeny, but further work is in progress to date the earlier deformation.

Several authors have noted that mylonitic rocks are characterized by fine grainsizes and represent zones of strain softening (Watterson 1975, White 1976, Etheridge & Wilkie 1979, White *et al.* 1980). The processes involved in strain softening constrain further deformation to the fine-grained mylonite and thus prevent the zone from widening. The ultramylonites within the Alice Springs region are thought to represent zones of extensive strain softening. The main processes involved, as indicated by the microstructural data, are (1) cyclic dynamic recrystallization, (2) geometrical softening and (3) reaction softening. The cyclic dynamic recrystallization ensures that there are always strain-free grains and leads to a finer grainsize. Geometric softening allows the rotation of slip planes into parallelism with the shear direction, and reaction softening, as seen within the amphibole bearing ultramylonites, produces a strain-free fine-grained weaker assemblage through metamorphic reactions.

Previous workers (White 1976, Rutter 1976, Etheridge & Wilkie 1979) have produced deformation maps for quartz which suggest that as grainsize is reduced there is a switch from dominantly dislocation-creep processes to diffusion mechanisms, including grain-boundary sliding. If this is the case for the ultramylonites in the present study, then the change in deformation mechanism would aid the softening processes and possibly lead to superplasticity.

Evidence for the operative deformation mechanisms was seen during the TEM analysis, where high dislocation densities were found in grainsizes down to 2 μm, in both the high-temperature ultramylonites containing hornblende and stable garnet, and the lower-temperature biotite–epidote-bearing ultramylonites. This observation suggests that dislocation processes were of continuing importance in the evolution of these rocks. Evidence for grain boundary sliding, on the other hand, is very limited, and considerable evidence against this mechanism is displayed within quartz vein rock. In the field, quartz veins crosscut the mylonitic foliation, but then became mylonitized themselves. These veins are therefore interpreted to represent the later stage during mylonitization, but nevertheless have been reduced to an ultrafine grainsize similar to that of the host ultramylonite. These monomineralic rocks exhibit a strong optical fabric when viewed with a sensitive tint plate (the orientation of the grains cannot be measured with a universal stage because of the exceptionally fine grainsize). Grain-boundary sliding in rocks, as well as in materials, is supposed to weaken preferred orientation (Boullier & Gueguen 1975), therefore it is not regarded as the dominant mechanism in the deformation of the monomineralic ultramylonites. It is uncertain whether this is equally applicable to the polymineralic specimens, although the presence of micas along grain boundaries may have aided the sliding processes. It therefore seems likely that deformation was accommodated by a complex interaction of dislocation processes in the larger grains, diffusion processes (which allow for the development of euhedral grains), and grain boundary sliding; but still we have inadequate knowledge of the deformation mechanisms.

One consequence of the formation of ultramylonites with ultrafine grainsizes is that the volume fraction of the grain boundaries and interphase boundaries increases relative to the volume fraction of the crystalline component. Gleiter (1981) in his review of ultrafine-grained materials, points out that a solid in which the volume of interfaces becomes comparable to the volume of the crystals may have differing structure and properties to the same material in the crystalline or amorphous state. This is due to the fact that the atoms are unable to relax to a structure of lowest free energy at grain boundaries. If this reasoning may be applied to ultrafine ultramylonites, which are likely to have grain boundaries with hydrated or distorted lattice films up to 30 nm thick (White & White 1981), then the formation of such a rock would have profound effects on continuing deformation or future reactivation.

Some of the ultramylonite bands, as described earlier, are considered to have been formed by a different mechanism, similar to that reported by Sibson (1980) and Passchier (1984). These bands have the sharpest

margins and finest grainsize and are considered to have originated as pseudotachylytes which have been subsequently refoliated and provide further suggestions that episodes of seismogenic slip occur during aseismic shearing within the deep crust.

The most noticeable characteristic of all the ultramylonites in the Alice Springs region is the fine grainsize. Observations have shown that there is little difference in grainsize between the higher and lower temperature bands. This suggests that temperature had negligible effects on the ultimate grainsize of these rocks, and places more emphasis on stress and strain rate. The fact that the grainsize has remained so fine after deformation is remarkable, and might be explained by second-phase particles (biotites) preventing the growth of quartz and feldspar. But this does not explain the fine grainsize of the mylonitized monomineralic quartz vein material.

CONCLUSIONS

From the microstructural evidence cited above it is concluded that the faults display a change from ductile to brittle deformation processes southwards in the Alice Springs region. This change is interpreted as a reflection of the progressive shallowing of the crustal deformation in the fault zones to the south. The northern fault zones were uplifted to higher crustal levels by the more southern faults. The textures of the fault rocks are thought to have developed during the Alice Springs Orogeny with localized areas within the Redbank Deformed Zone having mylonites belonging to earlier deformation events. Within the ultramylonites both metamorphic and deformational processes have given rise to strain softening. Deformation mechanisms at ultrafine grainsizes involve complex interactions of dislocation, diffusion and grain-boundary sliding processes.

Acknowledgements—Many thanks are due to Russell Shaw for his support and encouragement whilst in the field in Australia, and the hospitality and facilities offered by the Alice Springs Office of the N.T. Geological Survey were most appreciated. Thanks are also due to Louise for the typing of the original manuscript. HKO acknowledges financial support through a NERC Postgraduate Studentship and SHW thanks the Royal Society for support through an Anglo–Australian Fellowship and the University of Melbourne for a Visiting Fellowship. Electron microscopy was supported by NERC Grant GR3/3848.

REFERENCES

Armstrong, R. L. & Stewart, A. J. 1975. Rubidium–strontium dates and extraneous argon in the Arltunga Nappe Complex, Northern Territory. *J. geol. Soc. Aust.* **22**, 103–115.

Barber, D. J. 1970. Thin foils of non-metals made for electron microscopy by sputter etching. *J. Mater. Sci.* **5**, 1–8.

Black, L. P., Shaw, R. D. & Stewart, A. J. 1983. Rb–Sr geochronology of Proterozoic events in the Arunta Inlier, Central Australia. *BMR J. Aust. Geol. Geophys.* **8**, 129–137.

Boullier, A. M. & Gueguen, Y. 1975. S–P mylonites: origin of some mylonites by superplastic flow. *Contr. Miner. Petrol.* **50**, 93–104.

Brunel, M. 1980. Quartz fabrics in shear zone mylonites: evidence of a major imprint due to late strain increments. *Tectonophysics* **64**, T33–T44.

Etheridge, M. A. & Wilkie, J. C. 1979. Grain size reduction, grain boundary sliding and the flow strength of mylonites. *Tectonophysics* **58**, 159–178.

Evans, D. J. & White, S. H. 1984. Microstructural and fabric studies from the rocks of the Moine Nappe, Eriboll, NW Scotland. *J. Struct. Geol.* **6**, 369–389.

Gleiter, H. 1981. Materials with ultra-fine grain sizes. In: *Deformation of Polycrystals: Mechanisms and Microstructures* (edited by Hansen, N., Horsewell, A., Leffers, T. & Liholt, H.). Risø, Copenhavn, 15–21.

Hall, S. H. 1983. Post Alpine tectonic evolution of SE Spain and the structure of fault gouges. Unpublished Ph.D. thesis, University of London.

Iyer, S. S., Woodford, P. J. & Wilson, A. F. 1976. Rb–Sr isotopic studies of a polymetamorphic granulite terrain, Strangeways Range, Central Australia. *Lithos* **9**, 211–224.

Lister, G. S. 1977. Discussion: cross girdle *c*-axis fabrics in quartzites plastically deformed by plane strain and progressive simple shear. *Tectonophysics* **39**, 51–54.

Marjoribanks, R. W. 1974. The structural and metamorphic geology of the Ormistan region, Central Australia. Unpublished Ph.D. thesis, Australian National University.

Offe, L. A. & Shaw, R. D. 1983. Alice Springs Region—1:100,000 Geological Map Commentary. Bureau of Mineral Resources, Australia.

Passchier, C. W. 1982. Pseudotachylyte and the development of ultramylonite bands in the Saint Barthelemy Massif, French Pyrenees. *J. Struct. Geol.* **4**, 69–79.

Passchier, C. W. 1983. The reliability of asymmetric *c*-axis fabrics of quartz to determine sense of vorticity. *Tectonophysics* **99**, T9–T18.

Passchier, C. W. 1984. The generation of ductile and brittle shear bands in a low-angle mylonite zone. *J. Struct. Geol.* **6**, 273–281.

Platt, J. P. & Vissers, R. L. M. 1980. Extensional structures in anisotropic rocks. *J. Struct. Geol.* **2**, 397–410.

Rutter, E. H. 1976. The kinematics of rock deformation by pressure solution. *Phil. Trans. R. Soc.* **A283**, 203–219.

Shaw, R. D. & Wells, A. T. 1983. 1:250,000 Geological series—explanatory notes. Sheet SF/53-14, Bureau of Mineral Resources, Australia.

Sibson, R. H. 1977. Fault rocks and fault mechanisms. *J. geol. Soc. Lond.* **133**, 191–213.

Sibson, R. H. 1980. Transient discontinuities in ductile shear zones. *J. Struct. Geol.* **2**, 165–171.

Sibson, R. H. 1983. Continental fault structure and the shallow earthquake source. *J. geol. Soc. Lond.* **140**, 741–767.

Simpson, C. & Schmid, S. M. 1983. An evaluation of criteria to deduce the sense of movement in sheared rocks. *Bull. geol. Soc. Am.* **94**, 1281–1288.

Watterson, J. 1975. Mechanisms for the persistence of tectonic lineaments. *Nature, Lond.* **253**, 520–522.

White, S. H. 1976. The effects of strain on the microstructures, fabrics and deformation mechanisms in quartz. *Phil. Trans. R. Soc.* **A283**, 69–86.

White, S. H. 1982. Fault rocks of the Moine Thrust zone: a guide to their nomenclature. *Textures and Microstructures* **4**, 211–221.

White, S. H. & Knipe, R. J. 1978. Transformation- and reaction-enhanced ductility in rocks. *J. geol. Soc. Lond.* **135**, 513–516.

White, S. H., Burrows, S. E., Carreras, J., Shaw, N. D. & Humphreys, F. J. 1980. On mylonites in ductile shear zones. *J. Struct. Geol.* **2**, 175–187.

White, S. H., Shaw, H. F. & Huggett, J. M. 1984. The use of back-scattered electron imaging for the petrographic study of sandstones and shales. *J. sedim. Petrol.* **54** (2), 487–494.

White, J. C. & White, S. H. 1981. On the structure of grain boundaries in tectonites. *Tectonophysics* **78**, 613–628.

White, J. C. & White, S. H. 1983. Semi-brittle deformation within the Alpine Fault Zone, New Zealand. *J. Struct. Geol.* **5**, 679–689.